

Performance of Kinetic Energy Functionals for Interaction Energies in a Subsystem Formulation of Density Functional Theory

Andreas W. Götz,*^{†,‡} S. Maya Beyhan,[†] and Lucas Visscher*,[†]

*VU University Amsterdam, Theoretical Chemistry, De Boelelaan 1083,
1081 HV Amsterdam, The Netherlands*

Received April 11, 2009

Abstract: We have tested the performance of a large set of kinetic energy density functionals of the local density approximation (LDA), the gradient expansion approximation (GEA), and the generalized gradient approximation (GGA) for the calculation of interaction energies within a subsystem approach to density functional theory. Our results have been obtained with a new implementation of interaction energies for frozen-density embedding into the Amsterdam Density Functional program. We present data for a representative sample of 39 intermolecular complexes and 15 transition metal coordination compounds with interaction energies spanning the range from -1 to -783 kcal/mol. This is the first time that kinetic energy functionals have been tested for such strong interaction energies as the ligand–metal bonds in the investigated coordination compounds. We confirm earlier work that GGA functionals offer an improvement over the LDA and are particularly well suited for weak interactions like hydrogen bonds. We do, however, not find a particular reason to prefer any of the GGA functionals over another. Functionals derived from the GEA in general perform worse for all of the weaker interactions and cannot be recommended. An unexpectedly good performance is found for the coordination compounds, in particular with the GEA-derived functionals. However, the presently available kinetic energy functionals cannot be applied in cases in which a density redistribution between the subsystems leads to strongly overlapping subsystem electron densities.

1. Introduction

The quantum chemical study of large molecular systems which are of importance in life sciences or nanotechnology requires the use of multilevel methods which can treat different parts of the total system using different approximations. The frozen-density-embedding (FDE) scheme^{1,2} first developed by Wesolowski and Warshel is such a promising multilevel method. It has already been applied in a number of studies, for example,

of solvent effects on absorption spectra,^{3–5} electron spin resonance parameters,⁶ and nuclear magnetic resonance chemical shifts.⁷

FDE is based on a subsystem formulation⁸ of density functional theory (DFT),⁹ in which a large system is assembled from an arbitrary number of subsystems which are coupled by an effective embedding potential. In this way, the ground-state electron density is obtained as a superposition of subsystem electron densities, and the ground-state energy is obtained as a sum of subsystem energies and an interaction energy. FDE can be regarded as an approximation to Kohn–Sham (KS) DFT in which part of the kinetic energy of the noninteracting reference system is calculated via an explicit density functional. Making the theory formally exact therefore requires knowledge of the exact functional (T_S) for this energy in addition to the functional for the exchange-

* Corresponding author e-mail: agoetz@sdsc.edu (A.W.G.); visscher@chem.vu.nl (L.V.).

[†] VU University Amsterdam.

[‡] Current address: San Diego Supercomputer Center, University of California San Diego, 9500 Gilman Drive MC0505, La Jolla, California, 92037.

correlation (XC) energy that is already used in KS-DFT. In practice, one employs approximate functionals for both energy terms.

Although it is only a small fraction of the total kinetic energy which has to be approximated in FDE, the limited accuracy of available functionals puts severe restrictions on the possible partitioning of a system and limits the accuracy of numerical results which can be obtained with standard FDE calculations. In general, the error with respect to KS-DFT results becomes larger with increasing strength of the interactions between the subsystems. For example, the inclusion of covalent bonds between subsystems is at present only possible with an extension of the simple FDE scheme¹⁰ in which capping groups are introduced to improve the description.

Most published applications of FDE employ either the Thomas–Fermi (TF) kinetic energy functional^{11,12} or the generalized gradient approximation (GGA) functional PW91k,^{13,14} which have been shown to deliver good accuracy for subsystems with weak interactions and hydrogen bonds.^{14–21} Studies regarding the accuracy of kinetic energy functionals for FDE interaction energies, however, have either focused on one type of weak interactions for a small set of systems,^{14,22} been limited to a restricted number of approximate kinetic energy functionals,^{20,21} or both.^{14–16,19,23,24}

The aim of this contribution is to bridge this gap and provide a systematic analysis of the performance of existing kinetic energy functionals in the context of FDE. To this end, we have extended a flexible and efficient implementation²⁵ of FDE in the Amsterdam Density Functional program package (ADF)^{26–28} such that interaction energies can be computed. We have applied this implementation to a diverse range of data sets of molecular complexes covering not only weakly interacting and hydrogen-bonded systems but also transition metal complexes with coordination bonds.

In the next section, we sketch the aspects of the FDE formalism which are of importance for further discussion. Section 3 continues with a discussion of the form of the kinetic energy functionals which we have investigated in this study. In section 4, we present the data sets which we have used for assessing the performance of the kinetic energy functionals. Section 5 contains the computational details of our study. In section 6, we discuss the results which we have obtained with our implementation. We first analyze the convergence behavior of the interaction energies with respect to the optimization of the electron densities in the individual subsystems. Then, we assess the accuracy of FDE in combination with different kinetic energy functionals with respect to KS-DFT. Section 7 summarizes our findings.

2. Frozen-Density Embedding

The starting point for FDE^{1,2,25} is a subsystem formulation of DFT,⁸ in which the total system is partitioned into N subsystems such that the total electron density $\rho^{\text{tot}}(r)$ is represented as the sum of the subsystem electron densities $\rho^{(i)}(r)$:

$$\rho^{\text{tot}}(r) = \sum_i^N \rho^{(i)}(r) \quad (1)$$

with each subsystem containing a fixed integer number of electrons. The total electronic DFT energy for such a partitioning is most conveniently written as

$$E[\rho^{(1)}, \dots, \rho^{(N)}] = \sum_i^N E^{(i)}[\rho^{(i)}] + E_{\text{int}}[\rho^{(1)}, \dots, \rho^{(N)}] \quad (2)$$

where $E^{(i)}[\rho^{(i)}]$ is the standard KS-DFT total energy of subsystem i :

$$E^{(i)}[\rho^{(i)}] = T_s[\rho^{(i)}] + \int \nu_{\text{nuc}}^{(i)}(r) \rho^{(i)}(r) \, dr + \frac{1}{2} \int \frac{\rho^{(i)}(r) \rho^{(i)}(r')}{|r - r'|} \, dr \, dr' + E_{\text{xc}}[\rho^{(i)}] \quad (3)$$

Here, $\nu_{\text{nuc}}^{(i)}(r)$ is the electrostatic potential of the nuclei in subsystem i and $E_{\text{xc}}[\rho^{(i)}]$ is the XC energy of subsystem i . The interaction energy between the subsystems is then given as

$$E_{\text{int}}[\rho^{(1)}, \dots, \rho^{(N)}] = \sum_{i \neq j}^N \int \nu_{\text{nuc}}^{(i)}(r) \rho^{(j)}(r) \, dr + \sum_{i < j}^N \int \frac{\rho^{(i)}(r) \rho^{(j)}(r')}{|r - r'|} \, dr \, dr' + T_s^{\text{nad}}[\rho^{(1)}, \dots, \rho^{(N)}] + E_{\text{xc}}^{\text{nad}}[\rho^{(1)}, \dots, \rho^{(N)}] \quad (4)$$

where the nonadditive kinetic energy $T_s^{\text{nad}}[\rho^{(1)}, \dots, \rho^{(N)}]$ and the nonadditive XC energy $E_{\text{xc}}^{\text{nad}}[\rho^{(1)}, \dots, \rho^{(N)}]$ are defined as

$$T_s^{\text{nad}}[\rho^{(1)}, \dots, \rho^{(N)}] = T_s[\rho^{\text{tot}}] - \sum_i^N T_s[\rho^{(i)}] \quad (5)$$

and

$$E_{\text{xc}}^{\text{nad}}[\rho^{(1)}, \dots, \rho^{(N)}] = E_{\text{xc}}[\rho^{\text{tot}}] - \sum_i^N E_{\text{xc}}[\rho^{(i)}] \quad (6)$$

In these expressions, $T_s[\rho]$ is the kinetic energy of the reference system of noninteracting electrons, which can be calculated exactly if the KS orbitals are known for all densities. Within FDE, however, one would like to determine KS orbitals only for the individual subsystems. This goal can be realized by employing an approximate kinetic energy functional to evaluate $T_s^{\text{nad}}[\rho^{(1)}, \dots, \rho^{(N)}]$.

Minimization of the total energy functional of eq 2 with respect to the electron density $\rho^{(i)}$ of a subsystem i while keeping the electron density of all other subsystems frozen (fixed) leads to a set of coupled KS-like equations:

$$\left[-\frac{1}{2} \nabla^2 + \nu_{\text{eff}, \text{KS}}^{(i)}[\rho^{(i)}](r) + \nu_{\text{emb}}^{(i)}[\rho^{(1)}, \dots, \rho^{(N)}](r) \right] \psi_k^{(i)}(r) = \varepsilon_k^{(i)} \psi_k^{(i)}(r) \quad (7)$$

from which the KS orbitals $\{\psi_k^{(i)}\}$ and the associated electron density $\rho^{(i)}$ of subsystem i can be determined. The KS effective potential $\nu_{\text{eff}, \text{KS}}^{(i)}[\rho^{(i)}]$ contains the usual terms of the electrostatic potential of the nuclei, the Hartree potential, and

the XC potential of subsystem i . The effective embedding potential $\nu_{\text{emb}}^{(i)}[\rho^{(1)}, \dots, \rho^{(N)}]$ describes the effect of all other subsystems on subsystem i and reads

$$\begin{aligned} \nu_{\text{emb}}^{(i)}[\rho^{(1)}, \dots, \rho^{(N)}](r) = & \sum_{j,j \neq i}^N \int \nu_{\text{nuc}}^{(j)}(r) + \\ & \sum_{j,j \neq i}^N \int \frac{\rho^{(j)}(r')}{|r - r'|} dr' + \left. \frac{\delta E_{\text{xc}}[\rho]}{\delta \rho} \right|_{\rho=\rho^{\text{tot}}(r)} - \left. \frac{\delta E_{\text{xc}}[\rho]}{\delta \rho} \right|_{\rho=\rho^{(i)}(r)} + \\ & \left. \frac{\delta T_s[\rho]}{\delta \rho} \right|_{\rho=\rho^{\text{tot}}(r)} - \left. \frac{\delta T_s[\rho]}{\delta \rho} \right|_{\rho=\rho^{(i)}(r)} \quad (8) \end{aligned}$$

In addition to the electrostatic potential of the nuclei and electrons of the environment, it contains contributions from the nonadditive XC functional and the nonadditive kinetic energy functional.

In order to be able to yield the exact ground-state electron density ρ^{tot} , the subsystem electron density $\rho^{(i)} = \rho^{\text{tot}} - \sum_{j,j \neq i}^N \rho^{(j)}$ has to be positive and noninteracting ν -representable. In practice, it will be difficult to initialize the frozen subsystem densities such that the positivity condition for the active density is fulfilled. In such cases, the subsystem densities have to be determined in an iterative fashion.⁸ This can be achieved by so-called “freeze-and-thaw” cycles,²⁹ in which the electron density of one active subsystem is updated and then frozen again while the electron density of the next subsystem is determined. This procedure can be repeated in a self-consistent fashion until the electron densities of all subsystems are converged.

If the exact density functional for the KS kinetic energy $T_s[\rho]$ were known, the freeze-and-thaw procedure of FDE would represent an alternative way to determine the density of the total KS system. This means that convergence of this procedure should, irrespective of the employed XC functional, lead to the same ground state electron density and electronic ground state energy as with conventional KS-DFT (for the chosen XC functional). In an exact theory, it would thereby be possible to partition the density in different ways over the subsystems, the different choices resulting in differences in the individual subsystem energies that are compensated by differences in the interaction energy to yield a consistent total energy. [One could also think of a flexible setup in which the number of electrons on each subsystem is allowed to vary dynamically.] With the approximate kinetic energy functionals used in practical calculations, not all partitionings are meaningful, however. As a rule of thumb, one should avoid situations in which the subsystem densities overlap strongly and yield a large value of T_s^{nad} .³⁰ While this is easy to avoid for the starting densities, errors in the embedding potential may lead to an overestimation of charge transfer effects in a freeze-and-thaw optimization, bringing the partitioning outside the realm of applicability of the approximate functional.

3. Kinetic Energy Functionals

Several approximate types of kinetic energy functionals are available nowadays, and a comprehensive review is available in reference 31. An overview on the use of such functionals in FDE can be found, for example, in references 2 and 22. We therefore will restrict ourselves to a short overview on the functionals which we have investigated in this work. It

should therefore be noted that among others the TF functional was originally constructed to describe the total kinetic energy T rather than the KS kinetic energy T_s of the noninteracting reference system that is applicable when the correlation-kinetic energy T_c is implicitly included in the XC energy E_{xc} .³¹

We would, furthermore, like to point out that there does not seem to exist a correlation between the accuracy of approximate kinetic energy functionals for the total KS kinetic energy T_s and kinetic energy differences such as the nonadditive kinetic energy T_s^{nad} .^{2,30–32} For instance, some of the functionals investigated in this work fail to give binding of some simple molecules if used in orbital-free DFT with the correct KS density (for a given XC functional) as input.³³ However, this does not mean that these functionals will perform equally as bad if used to approximate only T_s^{nad} .

We have considered kinetic energy functionals which, for the general case of spin-polarized systems with spin density ρ_σ ($\sigma = \alpha, \beta$), can be written in the following form:

$$T_s^{\text{approx}}[\rho] = 2^{2/3} C_F \sum_{\sigma=\alpha,\beta} \int \rho_\sigma^{5/3}(r) F_T(s_\sigma(r)) dr \quad (9)$$

Here, $C_F = (3/10)(3\pi^2)^{2/3} \approx 2.871$ is the TF constant. $F_T(s_\sigma)$ denotes the enhancement factor, which is a function of the reduced density gradient

$$s_\sigma(r) = \frac{|\nabla \rho_\sigma(r)|}{2k_{F,\sigma}(r) \rho_\sigma(r)} \quad (10)$$

with the Fermi vector

$$k_{F,\sigma}(r) = [6\pi^2 \rho_\sigma(r)]^{1/3} \quad (11)$$

The analytic form of $F_T(s_\sigma)$ determines the gradient dependence of the approximate kinetic energy functional.

3.1. Local Density Approximation (LDA). Just as for the total kinetic energy, the dominant part of the nonadditive kinetic energy T_s^{nad} can be derived from the LDA, that is, TF theory.^{14,22} The TF enhancement factor is given as

$$F_{\text{TF}}(s_\sigma) = 1 \quad (12)$$

3.2. Gradient Expansion Approximation (GEA). For slowly varying electron densities, the kinetic energy can be represented by a gradient expansion^{34,35} in which TF theory represents the zeroth-order term. Truncation to second order yields the TF functional with von Weizsäcker correction, for which the enhancement factor takes the form

$$F_{\text{TF9W}}(s_\sigma) = 1 + \frac{5}{27} s_\sigma^2 \quad (13)$$

E00. A kinetic energy functional which represents the GEA up to fourth order and for which the enhancement factor takes the form

$$F_{\text{E00}}(s_\sigma) = \frac{135 + 28s_\sigma^2 + 5s_\sigma^4}{135 + 3s_\sigma^2} \quad (14)$$

has been proposed by Ernzerhof.³²

P92. Perdew proposed a functional which reproduces the GEA up to sixth order.³⁶ The enhancement factor

$$F_{\text{P92}}(s_\sigma) = \frac{1 + 88.3960s_\sigma^2 + 16.3683s_\sigma^4}{1 + 88.2108s_\sigma^2} \quad (15)$$

has the same functional form as the E00 enhancement factor and differs only in its parameters.

OL1 and OL2. On the basis of scaling properties of $T_s[\rho]$, Ou-Yang and Levy³⁷ proposed two kinetic energy functionals which replace fourth- and higher-order GEA terms with approximate, simple expressions. The corresponding enhancement factors take the following forms:

$$F_{\text{OL1}}(s_\sigma) = 1 + \frac{5}{27}s_\sigma^2 + \frac{C_4^{(1)}}{C_F}bs_\sigma \quad (16)$$

and

$$F_{\text{OL2}}(s_\sigma) = 1 + \frac{5}{27}s_\sigma^2 + \frac{C_4^{(2)}}{C_F} \frac{bs_\sigma}{(1 + 4bs_\sigma)} \quad (17)$$

where $b = 2(3\pi^2)^{1/3}$, $C_4^{(1)} = 6.77 \times 10^{-3}$ and $C_4^{(2)} = 8.87 \times 10^{-2}$.

3.3. Generalized Gradient Approximation (GGA). The GGA seems at present to be the most promising and successful route to approximate kinetic energy functionals. According to a conjecture of Lee, Lee, and Parr (LLP), the kinetic energy and the exchange energy can be considered “conjoint” such that kinetic energy functionals may be constructed using the same analytical function for the enhancement factor as used in GGA exchange energy functionals.³⁸ It should be kept in mind that this conjointness conjecture is not strictly correct.³³

LLP91. LLP suggested the use of the analytical form of the Becke (B88) exchange functional,³⁹ but reparametrized for the kinetic energy³⁸

$$F_{\text{LLP91}}(s_\sigma) = 1 + \alpha \frac{(2^{1/3}bs_\sigma)^2}{1 + \gamma(2^{1/3}bs_\sigma) \sinh^{-1}(2^{1/3}bs_\sigma)} \quad (18)$$

with $\alpha = 4.4188 \times 10^{-3}$ and $\gamma = 2.53 \times 10^{-2}$.

PW86. The Perdew–Wang (PW86) exchange functional⁴⁰ with enhancement factor

$$F_{\text{PW86}}(s_\sigma) = (1 + 1.296s_\sigma^2 + 14s_\sigma^4 + 0.2s_\sigma^6)^{1/15} \quad (19)$$

has been tested for the kinetic energy by Lacks and Gordon.⁴¹

PW91k. The functional which has been applied most widely in applications of FDE has been dubbed PW91k. It uses the analytic form of the enhancement factor of the Perdew–Wang (PW91) exchange functional⁴² with parameters optimized for the kinetic energy by Lembarki and Chermette (LC94).¹³ The application of this kinetic energy functional in the context of FDE was investigated by Wesolowski and co-workers,^{14,22} who analyzed both the original PW91 as well as the LC94 enhancement factor and found that both improved upon earlier functionals due to the better behavior of these functions at large values of s_σ .

$$F_{\text{PW91k}}(s_\sigma) = 1 + \frac{[A_2 - A_3 \exp(-A_4 s_\sigma^2)]s_\sigma^2 - B_1 s_\sigma^4}{1 + A_1 s_\sigma \sinh^{-1}(As_\sigma) + B_1 s_\sigma^4} \quad (20)$$

with $A_1 = 0.093907$, $A_2 = 0.26608$, $A_3 = 0.0809615$, $A_4 = 100.0$, $A = 76.320$, and $B_1 = 0.57767 \times 10^{-4}$.

TW02. The analytic form of the enhancement factor suggested by Becke⁴³ and used in the Perdew–Burke–Ernzerhof (PBE) functional^{44,45} has been reparametrized by Tran and Wesolowski to reproduce the kinetic energy of He and Xe atoms.⁴⁶ It is given as

$$F_{\text{TW02}}(s_\sigma) = 1 + \frac{\mu s_\sigma^2}{1 + (\mu/\kappa)s_\sigma^2} \quad (21)$$

with $\kappa = 0.8438$ and $\mu = 0.2319$.

T92. The kinetic energy functional of Thakkar⁴⁷

$$F_{\text{T92}}(s_\sigma) = 1 + \frac{\beta(2^{1/3}bs_\sigma)^2}{1 + \gamma(2^{1/3}bs_\sigma) \sinh^{-1}(2^{1/3}bs_\sigma)} - \frac{C_4(2^{1/3}bs_\sigma)}{1 + 4bs_\sigma} \quad (22)$$

with $\beta = 0.0055$ and $C_4 = 0.072$ uses a linear combination of the enhancement factor of the B88 exchange and OL2 kinetic energy functionals and has been fitted to the kinetic energy of 77 molecules.

PBE2, PBE3, and PBE4. A different route was taken by Karasiev et al.³³ They reparametrized kinetic energy functionals to better reproduce forces, that is, the shape of the KS potential energy surface instead of focusing on the accuracy of total energies. Although it cannot be expected that these functionals perform well for absolute energies, one might hope to obtain good relative energies (like the bond energies studied in this work). To investigate the feasibility of this ansatz, we have included these functionals in our study. The enhancement factors considered are of the two-parameter PBE form^{43–45} and the three- and four-parameter series expansions of the PBE form,⁴⁸ called PBE n ($n = 2, 3, 4$) in the following. They can be written as

$$F_{\text{PBE}n}(s_\sigma) = 1 + \sum_{i=1}^{n-1} C_i^{(n)} \left[\frac{s_\sigma^2}{1 + a_i^{(n)}s_\sigma^2} \right]^i \quad (23)$$

where $a^{(1)} = 0.2942$, $C_1^{(1)} = 2.0309$, $a^{(2)} = 4.1355$, $C_1^{(2)} = -3.7425$, $C_2^{(2)} = 50.258$, $a^{(3)} = 1.7107$, $C_1^{(3)} = -7.2333$, $C_2^{(3)} = 61.645$, and $C_3^{(3)} = -93.683$. Although the parameters have been determined for a very limited set of molecules, some transferability of the functionals was found when applied to CO, a molecule which was not included in the training set.³³

4. Data Sets

Truhlar and co-workers have recently suggested different sets of molecular complexes for testing XC functionals in KS-DFT. Some of these test sets have already been employed by Dulak and Wesolowski to assess the accuracy of FDE interaction energies for two combinations of XC and kinetic

energy functionals in FDE.²¹ They have confirmed older studies by Wesolowski and co-workers^{15,16,19,21,23,24} and shown that FDE can outperform KS-DFT for interaction energies if an appropriate combination of functionals for the XC energy and the nonadditive kinetic energy is chosen. It is clear, however, that these encouraging findings are the result of an error cancellation between the applied XC and kinetic energy functionals. The accuracy of FDE for a given combination of functionals with respect to highly accurate interaction energies derived from wave function-based methods is system-dependent. Comparison of the combinations (i) LDA for both XC and nonadditive kinetic energy and (ii) PW91⁴² as a XC functional and PW91k for the nonadditive kinetic energy has shown²¹ that, for hydrogen-, dipolar- and weakly bonded dimers combination (i) performs well, while combination (ii) performs worse or even qualitatively wrong. For π -stacking complexes and complexes with charge-transfer character, however, the situation is reversed, and combination (ii) yields results which are in better agreement with the reference data.

These results²¹ are important for practical purposes since they show for which type of systems we can expect maximum error cancellation with the combination of functionals under investigation. They do not, however, directly assess the performance of a given kinetic energy functional for FDE. With the exact kinetic energy functional, FDE should reproduce the KS-DFT results and not perform better. We therefore assess the accuracy of kinetic energy functionals for FDE by comparison to the corresponding KS-DFT results obtained with the same XC functional as in the FDE calculations.

We use Truhlar's NC31/05 data set of noncovalently bound molecular complexes with equilibrium geometries obtained from benchmark wave-function-based calculations.^{49,50} The strength of interactions in this data set covers the range up to 16.15 kcal/mol at the benchmark level of theory. We use the fixed geometries of the benchmark equilibrium structures of the monomers and dimers from this data set to analyze the accuracy of FDE interaction energies obtained with different kinetic energy functionals in comparison to the corresponding KS-DFT results. While KS-DFT with the presently available GGA XC functionals does not adequately describe interactions between the molecular fragments in this data set, which are dominated by dispersion forces, a comparison of FDE to supermolecular KS-DFT still allows us to assess the accuracy of the kinetic energy functionals. In addition, if the KS-DFT results are recovered by FDE, existing empirical corrections for dispersion forces like the very successful DFT-D correction⁵¹ can be added. The complexes in the NC31/05 data set are further subdivided into five groups:^{49,50}

- HB6/04 (hydrogen bond). $(\text{NH}_3)_2$, $(\text{HF})_2$, $(\text{H}_2\text{O})_2$, $\text{NH}_3 \cdots \text{H}_2\text{O}$, $(\text{HCONH}_2)_2$, and $(\text{HCOOH})_2$ (benchmark interaction energies ranging from -3.15 to -16.15 kcal/mol)
- CT7/04 (charge transfer). $\text{C}_2\text{H}_4 \cdots \text{F}_2$, $\text{NH}_3 \cdots \text{F}_2$, $\text{C}_2\text{H}_2 \cdots \text{ClF}$, $\text{HCN} \cdots \text{ClF}$, $\text{NH}_3 \cdots \text{Cl}_2$, $\text{H}_2\text{O} \cdots \text{ClF}$, and $\text{NH}_3 \cdots \text{ClF}$ (benchmark interaction energies ranging from -1.06 to -10.62 kcal/mol)

- DI6/04 (dipole interaction). $(\text{H}_2\text{S})_2$, $(\text{HCl})_2$, $\text{HCl} \cdots \text{H}_2\text{S}$, $\text{CH}_3\text{Cl} \cdots \text{HCl}$, $\text{HCN} \cdots \text{CH}_3\text{SH}$, and $\text{CH}_3\text{SH} \cdots \text{HCl}$ (benchmark interaction energies ranging from -1.66 to -4.16 kcal/mol)

- WI7/05 (weak interaction). HeNe , HeAr , $(\text{Ne})_2$, NeAr , $\text{CH}_4 \cdots \text{Ne}$, $\text{C}_6\text{H}_6 \cdots \text{Ne}$, and $(\text{CH}_4)_2$ (benchmark interaction energies ranging from -0.04 to -0.51 kcal/mol)

- PPS5/05 (π - π stacking). $(\text{C}_2\text{H}_2)_2$, $(\text{C}_2\text{H}_4)_2$, sandwich (S) $(\text{C}_6\text{H}_6)_2$, T-shaped (T) $(\text{C}_6\text{H}_6)_2$, and parallel-displaced (PD) $(\text{C}_6\text{H}_6)_2$ (benchmark interaction energies ranging from -1.34 to -2.78 kcal/mol)

In addition, we use the BP8/05 data set⁵² of stacking interactions in six nucleic acid base complexes and hydrogen-bonding interactions in two Watson–Crick (WC) type base pairs.

- BP8/05 (nucleobase pairs). Adenine–thymine (A \cdots T), guanine–cytosine (G \cdots C), antiparallel cytosine dimer (anti C \cdots C), displaced cytosine dimer (displ C \cdots C), parallel cytosine dimer (par C \cdots C), uracil dimer (U \cdots U), WC adenine–thymine (WC A \cdots T), and WC guanine–cytosine (WC G \cdots C) (benchmark interaction energies ranging from -2.45 to -28.80 kcal/mol)

In order to check the performance of the kinetic energy functionals for stronger interactions than contained in the databases listed above, we added data sets containing coordination compounds to the list of systems to be tested. For this purpose, we employ a data set consisting of five complexes of Zn^{2+} with simple inorganic ligands, which we will refer to as Zn5/08. The structures have been obtained from a data set which has recently been compiled by Amin and Truhlar for the purpose of testing the performance of density functionals.⁵³ As did those authors, we studied the dissociation of the complexes into the Zn^{2+} ion and the ligand and, in the case of $\text{Zn}(\text{OH})_2$, into $\text{Zn}(\text{OH})^+$ and OH^- .

- Zn5/08 (Zn^{2+} coordination complexes). $\text{Zn}(\text{NH}_3)^{2+}$, $\text{Zn}(\text{H}_2\text{O})^{2+}$, ZnOH^+ , $\text{Zn}(\text{OH})_2$, and $\text{Zn}(\text{SCH}_3)^+$ (benchmark interaction energies ranging from -96.83 to -428.18 kcal/mol)

Finally, we have put together a data set of transition metal coordination complexes with ligands of the spectrochemical series. In order to prevent problems with high-spin/low-spin splittings in transition metal complexes, which are in general difficult to treat accurately with DFT in any case, we focus on octahedral Cr(III) complexes, which in general have a quadruplet ground state due to the three unpaired electrons in the metal t_{2g} orbitals. The structures have been obtained as described in section 5, and we studied the interaction energies between the ligand L^{n-} and the corresponding $[\text{Cr}(\text{OH}_2)_5]^{3+}$ fragment, that is, the ligand bonding energies. The accuracy of these energies is indicative, for example, of the applicability to the study of ligand exchange reactions.

- Cr10/09. $[\text{Cr}(\text{OH}_2)_5\text{L}]^{(3-n)+}$, where n is the charge of the ligand L^{n-} and the ligands are (in order of increasing ligand field splitting parameter) I^- , Br^- , S^{2-} , Cl^- , F^- , OH^- , H_2O , NH_3 , NO_2^- , and CO (interaction energies ranging from -43.83 to -782.78 kcal/mol at the PBE/TZ2P level of theory)

5. Computational Details

All calculations were performed with a development version of the ADF program^{26–28} using the gradient-corrected PBE^{44,45} XC functional. We used the TZ2P basis set of the ADF basis set library, which is a triple- ζ valence/double- ζ core all-electron Slater basis augmented with two sets of polarization functions. The ADF default settings for the numerical integration grid and the self-consistent field (SCF) procedure were used. Geometries of the Cr(III) complexes were considered as converged if the maximum element of the gradient was below 10^{-4} au/Å.

For the FDE calculations, we used the approximate kinetic energy functionals described in section 3. We tested both a monomolecular expansion basis, denoted as FDE(m), in which only basis functions located on the active subsystem are used for the expansion of its KS orbitals, and a supermolecular (global) expansion basis, denoted as FDE(s), in which the basis functions of all subsystems are used for the expansion of the KS orbitals of the active subsystem.⁵⁴ In FDE(m) calculations, the numerical integration grid was centered on the active subsystem with only a few grid points added to deal with the singularities of the Coulomb potential at point nuclei of the frozen subsystem in close proximity to the active subsystem.⁴

Unless otherwise noted, all reported FDE energies have been converged to 10^{-5} au in the iterative solution of the FDE eqs (eq 7). Both KS-DFT and FDE(s) energies were corrected for the basis set superposition error (BSSE) with the counterpoise technique.⁵⁵

The setup and execution of all calculations and the subsequent data extraction and analysis were automatized with the help of PyADF,⁵⁶ which is a scripting framework for quantum chemistry realized in the Python⁵⁷ programming language. PyADF was also employed to handle the freeze-and-thaw iterations in the FDE calculations of the Cr(III) complexes since these can at present not be handled within ADF for open-shell systems.

5.1. Implementation Notes. The FDE energy evaluation according to eq 2 relies on the implementation of total KS-DFT energies in ADF. The FDE interaction energies [see eq 4] were obtained from a new implementation into ADF which builds on an earlier implementation by Wesolowski and Dulak⁵⁸ for the nonadditive kinetic energy T_s^{nad} and the nonadditive XC energy $E_{\text{xc}}^{\text{nad}}$. In the current implementation, the T_s^{nad} and $E_{\text{xc}}^{\text{nad}}$ contributions to the interaction energy and the embedding potential are obtained from exact (as opposed to fitted) densities to increase the numerical accuracy. New is the calculation of the remaining terms, out of which the electrostatic interaction energy between the electron densities (Coulomb energy) of the subsystems merits some comments. We use the shorthand notation

$$J[\rho^{(i)}, \rho^{(j)}] = \int \frac{\rho^{(i)}(r) \rho^{(j)}(r')}{|r - r'|} dr dr' \quad (24)$$

With Slater-type basis functions, these integrals cannot be calculated analytically. Therefore, in ADF, the electron densities are expanded into an auxiliary basis set of Slater functions.^{27,59} The electrostatic potential of these fitted electron densities

$$\tilde{\rho}^{(i)}(r) = \rho^{(i)}(r) - \delta\rho^{(i)}(r) \quad (25)$$

can be evaluated on the numerical integration grid so that we can compute the approximate Coulomb energy by numerical quadrature as

$$\begin{aligned} \tilde{J}[\rho^{(i)}, \rho^{(j)}] &= J[\rho^{(i)}, \tilde{\rho}^{(j)}] + J[\delta\rho^{(j)}, \tilde{\rho}^{(i)}] = J[\rho^{(j)}, \tilde{\rho}^{(i)}] + \\ &\quad J[\delta\rho^{(i)}, \tilde{\rho}^{(j)}] \end{aligned} \quad (26)$$

$\tilde{J}[\rho^{(i)}, \rho^{(j)}]$ has an error of $\mathcal{O}(\delta\rho^{(i)}\delta\rho^{(j)})$.⁶⁰ An integration grid in the region of subsystems i and j is required in order to evaluate the integrals of eq 26. In FDE(m) calculations, however, efficiency reasons make it advantageous to center the numerical integration grid on the active subsystem. We therefore proceed as follows. Let us assume that we commence the n th freeze-and-thaw cycle and we optimize electron density $\rho^{(i)}(n)$ in the presence of all other subsystem electron densities $\rho^{(j)}(n-1)$ of the previous freeze-and-thaw iteration. We now compute $J[\rho^{(i)}(n), \tilde{\rho}^{(j)}(n-1)]$ and $J[\delta\rho^{(i)}(n), \tilde{\rho}^{(j)}(n-1)]$ using the grid of subsystem i and take $J[\rho^{(j)}(n-1), \tilde{\rho}^{(i)}(n-1)]$ and $J[\delta\rho^{(j)}(n-1), \tilde{\rho}^{(i)}(n-1)]$ from the $(n-1)$ th iteration (computed on a grid of subsystem j) to obtain an approximate Coulomb energy:

$$\tilde{J}[\rho^{(i)}, \rho^{(j)}](n) = \frac{1}{2}\{\tilde{J}'[\rho^{(i)}, \rho^{(j)}](n) + \tilde{J}''[\rho^{(i)}, \rho^{(j)}](n)\} \quad (27)$$

where

$$\begin{aligned} \tilde{J}'[\rho^{(i)}, \rho^{(j)}](n) &= J[\rho^{(i)}(n), \tilde{\rho}^{(j)}(n-1)] + \\ &\quad J[\delta\rho^{(j)}(n-1), \tilde{\rho}^{(i)}(n-1)] \end{aligned} \quad (28)$$

and

$$\begin{aligned} \tilde{J}''[\rho^{(i)}, \rho^{(j)}](n) &= J[\rho^{(j)}(n-1), \tilde{\rho}^{(i)}(n-1)] + \\ &\quad J[\delta\rho^{(i)}(n), \tilde{\rho}^{(j)}(n-1)] \end{aligned} \quad (29)$$

Upon convergence of the freeze-and-thaw cycles, eqs 28 and 29 become equivalent, and the difference

$$\Delta\tilde{J}[\rho^{(i)}, \rho^{(j)}](n) = |\tilde{J}'[\rho^{(i)}, \rho^{(j)}](n) - \tilde{J}''[\rho^{(i)}, \rho^{(j)}](n)| \quad (30)$$

has to vanish.

6. Results and Discussion

6.1. Convergence Behavior of Energy Contributions.

In Table 1, we show typical examples of the convergence behavior of the FDE energy (eq 2) during the iterative solution of the FDE eqs (eq 7). The error $\Delta\tilde{J}$ in the Coulomb energy [see eq 30] drops quickly to 10^{-6} au after the third to fourth freeze-and-thaw iteration, and at the same time, the energy converges to 10^{-5} au. It takes one additional iteration to converge FDE(s) calculations to the same accuracy as FDE(m) calculations.

We have observed a similar convergence behavior of FDE(m) calculations for all of the molecular complexes investigated, independent of the applied kinetic energy functional. Exceptions are the PBE_n functionals which caused SCF convergence problems in FDE(m) calculations for some of the transition metal complexes.

Table 1. Convergence Behavior of FDE Energy Terms (in au without BSSE correction) with the Number, n , of Freeze-and-Thaw Iterations for Two Representative Examples^a

FDE(m)					FDE(s)			
n	$\tilde{J}(n)$	$\Delta\tilde{J}(n)$	$E_{\text{int}}(n)$	$E(n)$	$\tilde{J}(n)$	$\Delta\tilde{J}(n)$	$E_{\text{int}}(n)$	$E(n)$
$\text{NH}_3 \cdots \text{H}_2\text{O}$								
1	17.639472	0.006771	-0.009632	-132.904592	17.646163	0.011736	-0.009104	-132.903440
2	17.633830	0.000169	-0.012977	-132.907889	17.643158	0.000663	-0.014824	-132.908967
3	17.633686	0.000003	-0.013064	-132.907978	17.642992	0.000032	-0.015151	-132.909281
4	17.633680	0.000007	-0.013066	-132.907977	17.642982	0.000005	-0.015169	-132.909302
5					17.642982	0.000007	-0.015171	-132.909300
$(\text{HCOOH})_2$								
1	93.989199	0.003520	-0.039358	-379.324115	94.034378	0.001900	-0.048987	-379.329414
2	93.985858	0.000203	-0.042262	-379.325771	94.034852	0.000137	-0.052773	-379.330506
3	93.985663	0.000015	-0.042440	-379.325864	94.035125	0.000029	-0.053048	-379.330448
4	93.985649	0.000001	-0.042452	-379.325870	94.035163	0.000004	-0.053075	-379.330436
5	93.985648	0.000000	-0.042453	-379.325869	94.035169	0.000002	-0.053078	-379.330429
					94.035169	0.000000	-0.053078	-379.330430

^a The PW91k functional was used for the nonadditive kinetic energy.

The convergence behavior of FDE(s) calculations, however, depends strongly on the type of intermolecular interactions and the kinetic energy functional employed. In general, FDE(s) calculations with LDA and GGA functionals (except PBE n) converge smoothly, with some exceptions. Around 25 freeze-and-thaw iterations were required for a converged FDE(s) energy of the charge-transfer complex $\text{NH}_3 \cdots \text{ClF}$, and with the LLP91 GGA functional no convergence could be obtained at all. Almost none of the Cr(III) complexes could be converged with FDE(s), irrespectively of the applied functional. The H_2O complex could be converged with the TF, PW91k, and TW02 functionals and the CO complex with the TF and PW91k functionals.

We encountered SCF convergence problems (either immediately or after some freeze-and-thaw iterations) with FDE(s) calculations employing kinetic energy functionals derived from the GEA (TF9W, E00, P92, OL1, OL2, T92) or the PBE n kinetic energy functionals for some of the complexes of the CT7/04, DI6/04, PPS/05, BP8/05, and Zn5/08 data sets and all complexes of the Cr10/09 data set (see also next section). This holds in particular for the E00, PBE2, and PBE4 functionals. Whenever good SCF convergence was achieved, however, the FDE(s) energy converged well within a few freeze-and-thaw iterations also for these functionals.

In the cases in which no convergence could be achieved, the functional derivative of the kinetic energy functional which enters the embedding potential [see eq 8] obviously leads to a qualitatively wrong potential. This does not necessarily lead to a problem in FDE(m) calculations. The availability of the full basis set for FDE(s), however, allows the electron density to probe regions where the embedding potential is too attractive.⁶¹ As a consequence, the electron density may redistribute, and the initially chosen subsystem partitioning can get lost such that the system enters the strong overlap regime and the approximate functional in use no longer is able to describe the situation.

Let us illustrate this with the example of an FDE(s) calculation with the TF functional for the $[\text{Cr}(\text{OH}_2)_5\text{F}]^{2+}$ complex, which is partitioned into $[\text{Cr}(\text{OH}_2)_5]^{3+}$ and F^- . Table 2 shows the Mulliken charges⁶² associated with the chromium and fluorine atoms in the two subsystems during

Table 2. Mulliken Charges Associated with the Fluorine and Chromium Atoms in the Two Subsystems of $[\text{Cr}(\text{OH}_2)_5\text{F}]^{2+}$ during the Course of Freeze-and-Thaw Iterations^a

freeze-and-thaw cycle	[$\text{Cr}(\text{OH}_2)_5$] ³⁺ subsystem		F ⁻ subsystem	
	Cr	F	Cr	F
0	1.5			-1.0
1	1.8	0.0	-0.2	-0.8
2	2.0	0.0	-0.3	-0.7
3	2.0	0.0	-0.5	-0.5
4	2.1	0.0	-1.2	0.3
5	2.2	0.0	-1.8	0.9

^a The TF functional was used as nonadditive kinetic energy functional.

the course of freeze-and-thaw iterations. We start out with a chromium atom which carries a charge of 1.5. The remaining charge of 1.5 is buffered by the water ligands. The fluoride atom has of course a charge of -1. What we then observe is a gradual transfer of density from the fluoride to the metal center during the course of the freeze-and-thaw iterations. Some charge transfer, accompanied by some back-bonding from the metal to the ligand, is to be expected during the formation of the coordination bond. However, in this case, too much density moves from the ligand to the metal center. As a consequence, after a few freeze-and-thaw iterations, a subsystem partitioning with strongly overlapping subsystem electron densities is reached, and results become meaningless.

6.2. Accuracy of Interaction Energies. We will discuss the accuracy of FDE interaction energies obtained with the different kinetic energy functionals for each data set, which represents a particular type of interaction, separately. In general, however, we found distinct performance for the LDA, for the group of functionals which are derived from the GEA (TF9W, E00, P92, OL1, OL2), standard GGA functionals (LLP91, PW86, PW91k, TW02), and the PBE n functionals. As could be expected from its functional form, the accuracy of the T92 functional is usually in between the accuracy of the GEA-derived functionals and that of the GGA functionals.

Figures 1 and 2 summarize the accuracy of the different kinetic energy functionals in FDE(m) and FDE(s) calcula-

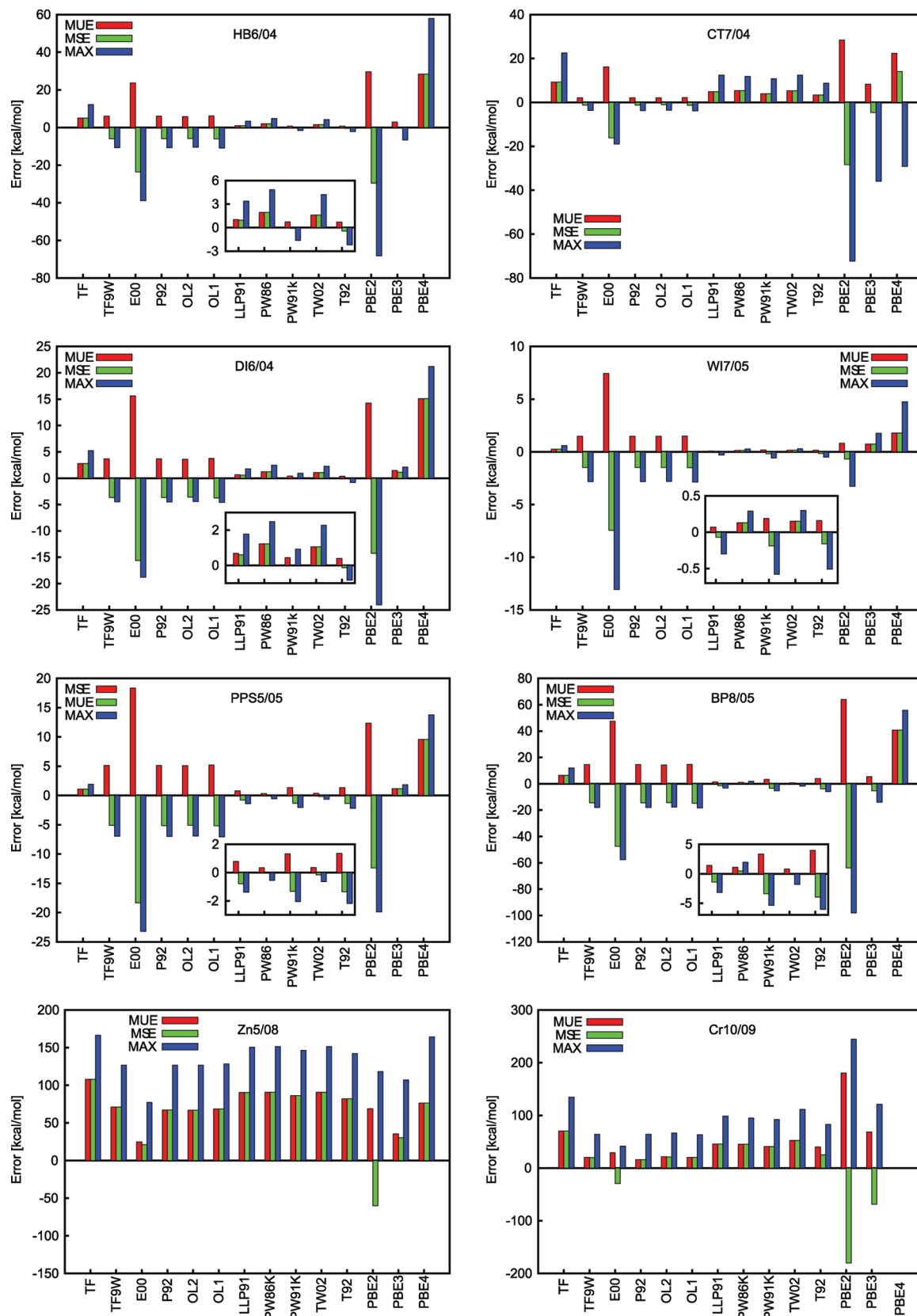


Figure 1. Performance of kinetic energy functionals for FDE(m) interaction energies for all investigated data sets. Mean unsigned error (MUE), mean signed error (MSE), and maximum error (MAX) for BSSE-corrected interaction energies.

tions, respectively, for all data sets investigated. No data are presented for the Cr10/09 data set with FDE(s) since essentially none of the calculations could be converged (see also section 6.1). Tables containing all interaction energies

for supermolecular KS-DFT, FDE(m), and FDE(s) can be found in the Supporting Information.

Figures 3 and 4 show a comparison of KS and FDE(m) interaction energies and KS and FDE(s) interaction energies,

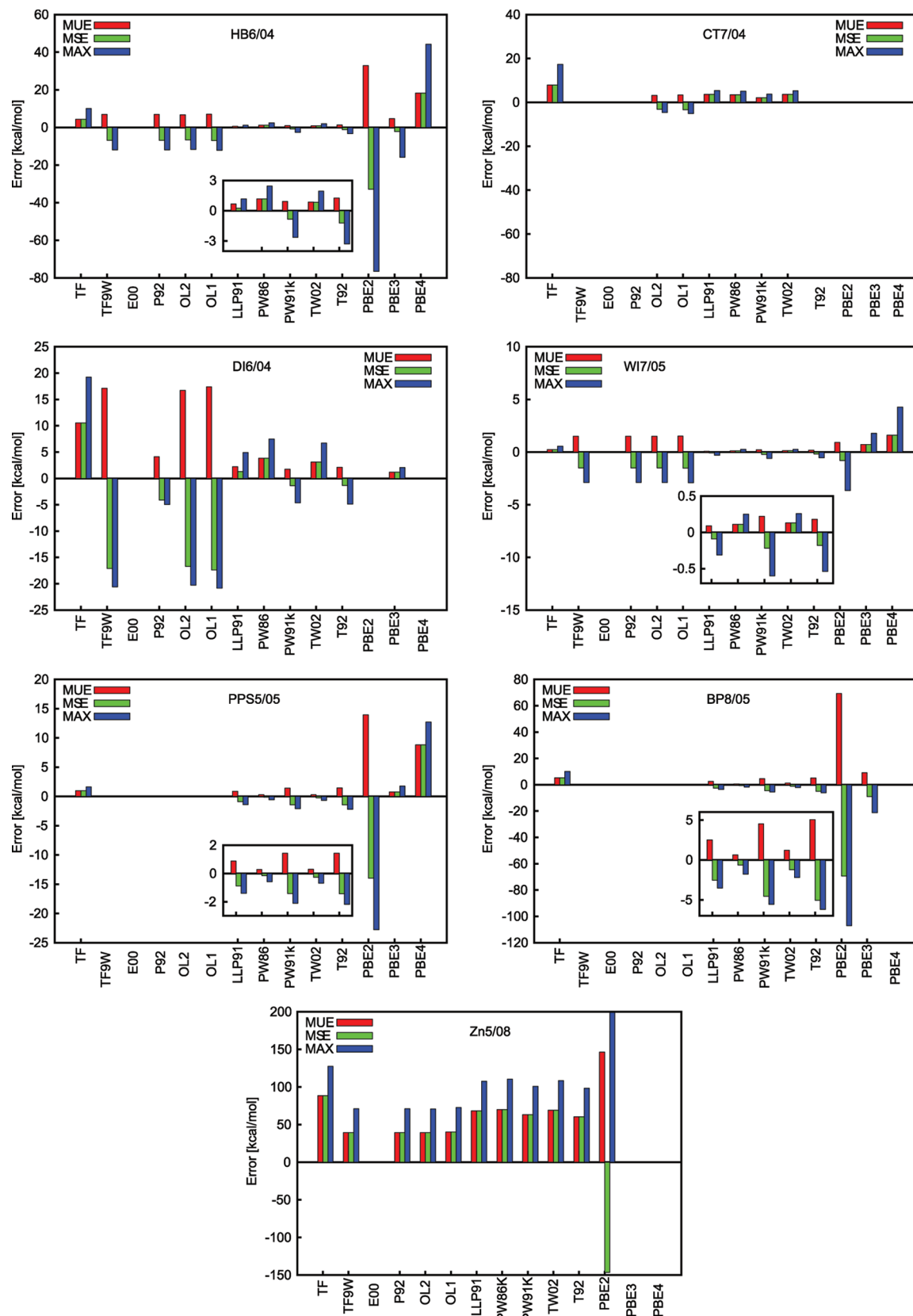


Figure 2. Performance of kinetic energy functionals for FDE(s) interaction energies for all investigated data sets. Mean unsigned error (MUE), mean signed error (MSE), and maximum error (MAX) of BSSE-corrected interaction energies.

respectively, for the three kinetic energy functionals which perform best for a given data set.

When discussing the performance of the kinetic energy functionals for the FDE interaction energies, one has to keep in mind that it is not only the form of the approximate

functional for the kinetic energy which determines the quality of the results. It is the functional derivative of the kinetic energy functional which enters the expression for the embedding potential [see eq 8] and as such determines the quality of the electron density obtained. It may well be

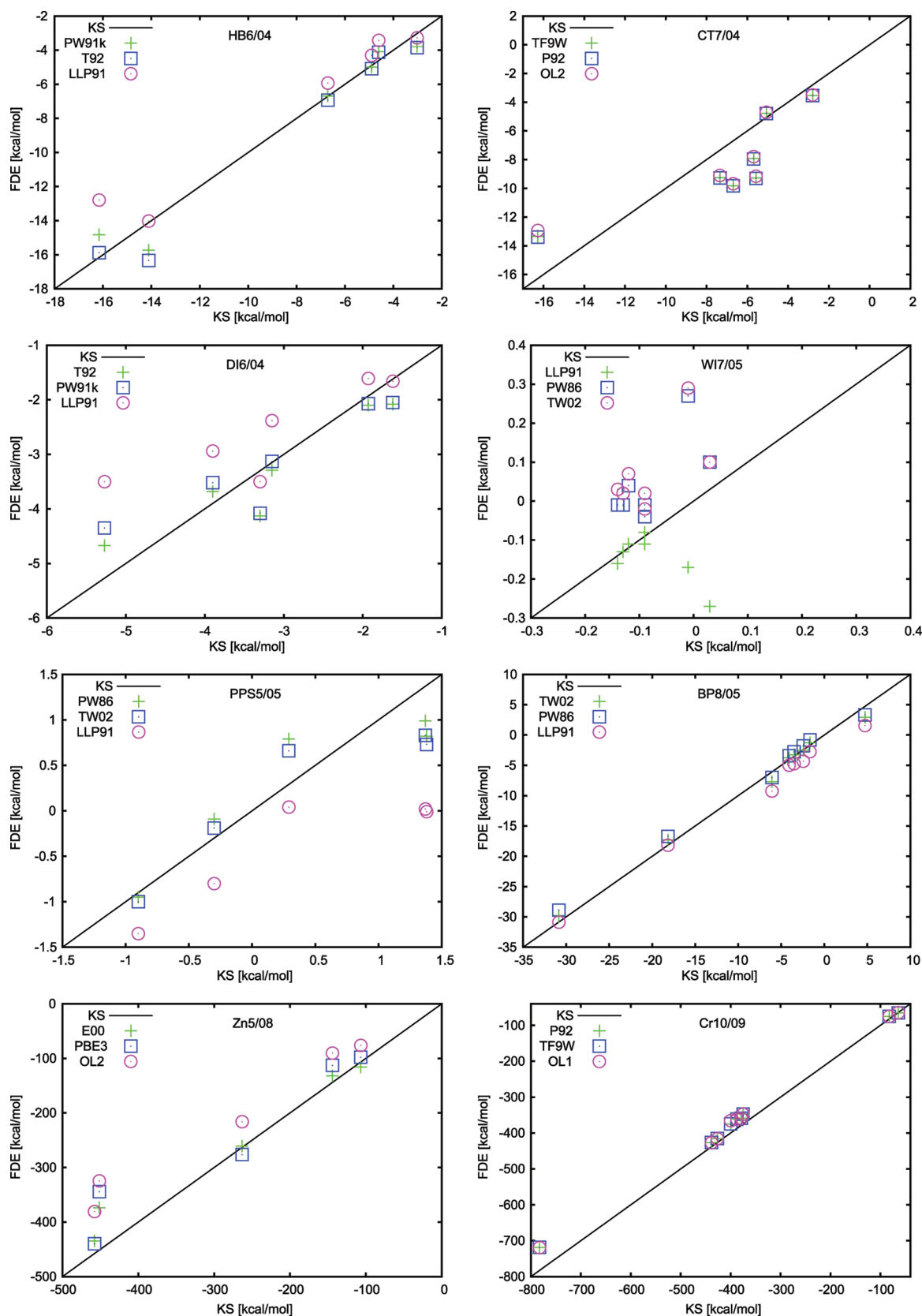


Figure 3. Comparison of KS interaction energies with those of FDE(m) for the kinetic energy functionals which have the smallest mean unsigned error (MUE) for a given data set.

the case that error cancellations happen in the sense that a good interaction energy is obtained, although the underlying electron density obtained from the preceding FDE calculation is not good at all.

From the point of view of computational efficiency, FDE(m) is clearly superior to FDE(s), the latter even having a higher computational cost than a corresponding supermolecular KS-DFT calculation. However, while

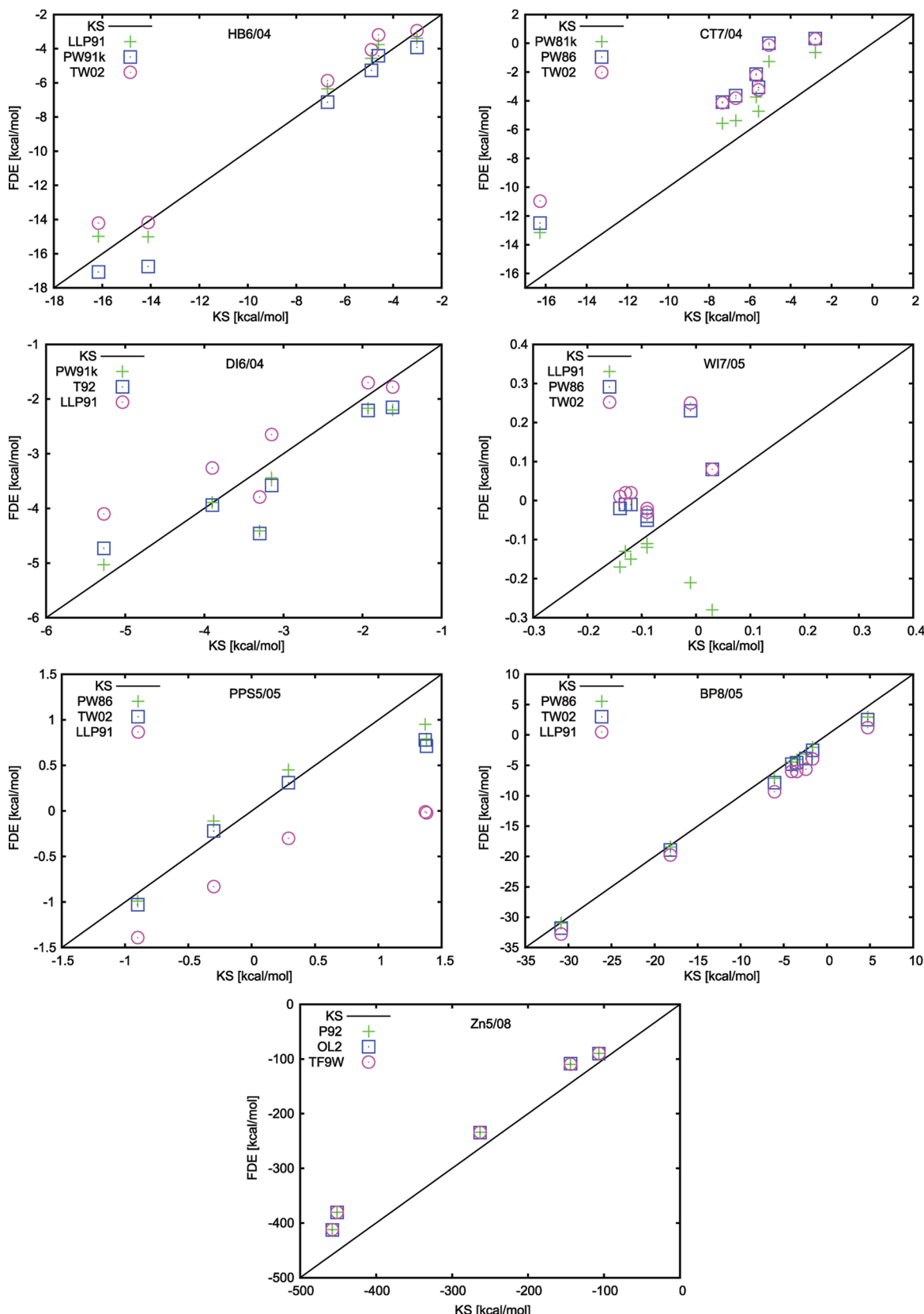


Figure 4. Comparison of KS interaction energies with those of FDE(s) for the kinetic energy functionals which have the smallest mean unsigned error (MUE) for a given data set.

FDE(m) allows for polarization of the subsystem electron densities, no charge transfer between the subsystems can be described with FDE(m). We would like to stress that only FDE(s) can exactly recover the results of a supermolecular KS-DFT calculation (with the unknown, exact

kinetic energy functional for the nonadditive kinetic energy T_s^{nad}). Thus, the proper reference for judging the accuracy of kinetic energy functionals for the nonadditive kinetic energy T_s^{nad} within the FDE formalism must be the results from FDE(s) calculations. However, in general,

whenever there is no net charge transfer between the subsystems, FDE(m) is an excellent approximation to FDE(s). This holds in particular if a sufficiently good basis set is employed which allows for a proper polarization of the subsystem electron densities. This certainly holds for the large TZ2P basis set employed in our studies.

Very good results are obtained for the interaction energies of the hydrogen-bonded dimers in the HB6/04 data set with the standard GGA functionals and the T92 functional, both with FDE(m) and FDE(s). The PW91k functional performs best for FDE(m) calculations, while the LLP91 functional takes the lead for FDE(s) calculations. Overall, however, the difference between these functionals is not big, and there is no clear reason to prefer one over another. The LDA performs much worse. It consistently underestimates the magnitude of the binding energies and cannot be recommended for energetics in hydrogen-bonded systems. The GEA-derived functionals offer no improvement over the LDA and consistently overshoot the binding energy. The PBE_n functionals perform particularly badly, with the exception of the PBE3 functional which, however, shows an unacceptably large maximum error in the case of FDE(s).

For the CT7/04 data set, the LDA performs very badly and does not predict any binding both for FDE(m) and for FDE(s). The GEA-derived functionals apart from E00 perform rather well for FDE(m); however, this must be due to an error cancellation because FDE(m) calculations are not able to model a real charge transfer. For FDE(s) calculations, in which such charge transfer is possible, similar performance is found, except for the TF9W functional for which the SCF could not be converged for some dimers. This is due to a too strong charge transfer due to errors in the embedding potential as discussed above. Acceptable results are also obtained with the standard GGA functionals for FDE(s), PW91k taking the lead. The PBE_n functionals perform very badly, again.

For the DI6/04 data set, very good results are obtained again with the standard GGA functionals, in particular, PW91k, but T92 is as good. Also, the PBE3 functional is able to deliver good results. Given the relatively small interaction energies, the LDA and GEA-derived functionals do not perform well, the errors being as large as the bonding energies. All functionals perform worse with FDE(s), indicating that some errors in the embedding potential are not probed by the smaller FDE(m) basis.

The intermolecular interactions in the WI7/05 data set are very weak, and most of the functionals perform similarly, both for FDE(m) and for FDE(s) calculations. Again, the standard GGA functionals and T92 give the best agreement with supermolecular KS-DFT calculations. Results obtained with the GEA-derived functionals and the PBE_n functionals in general have an error which is larger than the interaction energies themselves.

The interaction energies of the PPS5/05 data set are also rather weak, and it should be mentioned that KS-DFT does not predict any binding of the benzene dimers. The picture is similar to that for the other data sets, the standard GGA functionals performing best. Out of these, PW86 and TW02 are clearly superior, and PW91k has the largest errors. Also,

the LDA and the PBE3 functional give interaction energies relatively close to the KS-DFT results. The GEA-derived functionals and PBE2 and PBE4, however, yield useless results or, in the case of FDE(s), do not even converge.

For the BP8/05 data set, a similar picture as before arises. The GGA functionals and T92 perform rather well. Among these, PW91k shows the largest errors in the interaction energies. PW86 and TW02 are the most reliable functionals for these types of interactions. The LDA and the PBE3 functional still yield somewhat reasonable results. All other functionals either do not converge or show errors which are too large to make them useful for any practical interaction energy calculations.

At first sight, rather poor results are obtained for the Zn5/08 data set with very large maximum and mean errors. Given the strong interactions between the subsystems, however, the relative errors are much smaller than one might have expected. Due to the charge on the Zn²⁺ ion and the dipole moment or charge on the ligands, the interaction energy is dominated by the electrostatic contribution [nuclear–nuclear repulsion and first two terms of eq 4]. It is important to point out that the nonadditive kinetic energy contribution to the interaction energy is on the same order of magnitude as the electrostatic contribution. For instance, in an FDE(m) calculation on [Zn(OH)]⁺ with the E00 functional, the electrostatic contribution to the interaction energy of eq 4 between Zn²⁺ and OH⁻ is -623.73 kcal/mol, while the contribution due to the nonadditive kinetic and XC energy is +145.50 and -44.67 kcal/mol, respectively. This emphasizes the importance of a proper treatment of the nonadditive kinetic energy. Except for PBE2, all functionals underestimate the binding energies. For FDE(m), E00 performs best, and PBE3 is able to deliver better results than any other GGA functional. For FDE(s), however, one hits the problem described in section 6.1, and the SCF does not converge for any of the systems both with E00 and PBE3 as well as PBE4. It is particularly disappointing that GGA functionals do not bring a significant improvement over the LDA. As to be expected, for the cases in which the SCF converges, the FDE(s) results are in better agreement with the supermolecular KS-DFT calculations. Here, all GEA-derived functionals apart from E00 prove to be superior to other functionals. Unlike the other functionals, PBE2 overshoots the interaction energy for FDE(s) and exhibits particularly large errors. Nevertheless, it is encouraging to see (Figures 3 and 4) that the relative strength of the interaction energies is correctly reproduced by the best FDE calculations and, as mentioned above, the relative errors are rather small.

As already discussed in section 6.1, almost none of the complexes from the Cr10/09 data set could be converged with FDE(s). In the cases in which convergence was achieved, however, FDE(s) leads to an improvement over FDE(m) (see Supporting Information) with the exception of the CO complex for which the FDE(m) interaction energy with the PW91k functional is in better agreement with the supermolecular KS-DFT result. The FDE(m) results for the Cr10/09 data set are surprisingly good for most of the functionals, with the exception of the PBE_n series, which, again, performs rather poorly. In particular with PBE4, SCF

convergence could be achieved only for the fluoride complex. All functionals apart from E00 and PBE_n underestimate the binding energies. The best results are obtained with the GEA-derived functionals, out of which E00 is the worst. But also the GGA functionals apart from PBE_n still yield satisfactory interaction energies. At this point, it is important to note that, as for the Zn²⁺ coordination compounds, the electrostatic and nonadditive kinetic energy contributions to the FDE interaction energy are on the same order of magnitude and one order of magnitude larger than the nonadditive XC energy contribution. Thus, also here, the good correlation between KS and FDE interaction energies (Figure 3) is not only due to electrostatic interactions between the charged [Cr(H₂O)₅]³⁺ complex and ligand fragments. The nonadditive kinetic-energy functional plays a very important role.

7. Conclusions

We have implemented the calculation of interaction energies in the framework of FDE into the ADF program package. Using this implementation, we have performed a systematic analysis of the performance of a large set of LDA, GEA-derived, and GGA kinetic energy density functionals for the nonadditive kinetic energy contribution to FDE interaction energies. We have studied a representative data set with interaction energies ranging from -1 kcal/mol in weakly interacting dimers to -783 kcal/mol in coordination bonds of transition metal complexes.

We have shown that the freeze-and-thaw cycle for a self-consistent update of the subsystem electron densities and the accompanying FDE energy converges within a few iterations whenever the SCF of an FDE calculation converges smoothly. This is in general the case both for FDE(m) and for FDE(s) calculations with LDA and GGA kinetic-energy functionals, except for the PBE_n functionals. FDE(m) calculations with the GEA-derived and PBE_n-GGA functionals also converge properly. In FDE(s) calculations, however, convergence problems are encountered frequently with these functionals and, in the case of the Cr(III) complexes, for all functionals we have tested. Particularly bad in this respect are the E00, PBE2, and PBE4 functionals. Qualitatively wrong embedding potentials are obtained in these cases, which lead to strongly overlapping subsystem electron density partitionings which lie outside the domain of applicability of these approximate functionals.

Reasonable interaction energies can already be obtained with the LDA. However, GGA kinetic-energy functionals (apart from PBE_n) in general significantly improve upon the LDA. Exceptions are the very weak interactions of the WI7/05 data set and the coordination bonds in the Zn5/08 data set for which the errors with the LDA and GGA functionals are practically of equal magnitude. In most cases, the LLP91, TW02, and PW91k functionals work best, but there is no strong indication to prefer one GGA over another if interaction energies are the target of interest. Also, the PBE3 functional yields very good interaction energies in many cases, but it is not reliable, in particular for FDE(s) calculations for which no SCF convergence can be achieved in some cases.

It is particularly encouraging that reasonable results can be obtained for the bond energies in coordination compounds. In contrast to the weak intermolecular interactions, for these systems, the GEA-derived functionals perform better than the GGA functionals. This indicates that FDE using these functionals may be useful for studies of ligand exchange reactions or catalytic reactions in which transition metal centers are involved.

We expect our results to be transferable to FDE calculations carried out in conjunction with XC functionals other than PBE which we have employed throughout this work.

Acknowledgment. This work has been supported by NWO in form of a VICI grant for L.V.

Supporting Information Available: Tables containing interaction energies for supermolecular KS-DFT, FDE(m), and FDE(s) calculations for all investigated data sets. This information is available free of charge via the Internet at <http://pubs.acs.org/>.

References

- (1) Wesolowski, T. A.; Warshel, A. *J. Phys. Chem.* **1993**, *97*, 8050–8053.
- (2) Wesolowski, T. A. One-Electron Equations for Embedded Electron Density: Challenge for Theory and Practical Payoffs in Multi-Level Modelling of Complex Polyatomic Systems. In *Computational Chemistry: Reviews of Current Trends*; Leszczynski, J., Ed.; World Scientific: River Edge, NJ, 2006; Vol. 10, Chapter 1, pp 1–82.
- (3) Neugebauer, J.; Louwerse, M. J.; Baerends, E. J.; Wesolowski, T. A. *J. Chem. Phys.* **2005**, *122*, 094115.
- (4) Neugebauer, J.; Jacob, C. R.; Wesolowski, T. A.; Baerends, E. J. *J. Phys. Chem. A* **2005**, *109*, 7805–7814.
- (5) Jacob, C. R.; Neugebauer, J.; Jensen, L.; Visscher, L. *Phys. Chem. Chem. Phys.* **2006**, *8*, 2349–2359.
- (6) Neugebauer, J.; Louwerse, M. J.; Belanzoni, P.; Wesolowski, T. A.; Baerends, E. J. *J. Chem. Phys.* **2005**, *123*, 114101.
- (7) Jacob, C. R.; Visscher, L. *J. Chem. Phys.* **2006**, *125*, 194104.
- (8) Cortona, P. *Phys. Rev. B* **1991**, *44*, 8454–8458.
- (9) Parr, R. G.; Yang, W. *Density-Functional Theory of Atoms and Molecules*; Oxford University Press: Oxford, U. K., 1989.
- (10) Jacob, C. R.; Visscher, L. *J. Chem. Phys.* **2008**, *128*, 155102.
- (11) Thomas, L. H. *Proc. Camb. Phil. Soc.* **1927**, *23*, 542.
- (12) Fermi, E. *Rend. Accad. Lincei* **1927**, *6*, 602.
- (13) Lembarki, A.; Chermette, H. *Phys. Rev. A* **1994**, *50*, 5328–5331.
- (14) Wesolowski, T. A. *J. Chem. Phys.* **1997**, *106*, 8516–8526.
- (15) Wesolowski, T. A.; Ellinger, Y.; Weber, J. *J. Chem. Phys.* **1998**, *108*, 6078–6083.
- (16) Wesolowski, T. A.; Tran, F. *J. Chem. Phys.* **2003**, *118*, 20072–2080.
- (17) Wesolowski, T. A. *J. Am. Chem. Soc.* **2004**, *126*, 11444–11445.
- (18) Jacob, C. R.; Wesolowski, T. A.; Visscher, L. *J. Chem. Phys.* **2005**, *123*, 174104.
- (19) Kevorkyants, R.; Dulak, M.; Wesolowski, T. A. *J. Chem. Phys.* **2007**, *124*, 024104.

- (20) Dulak, M.; Kaminski, J. W.; Wesolowski, T. A. *J. Chem. Theory Comput.* **2007**, *3*, 735–745.
- (21) Dulak, M.; Wesolowski, T. A. *J. Mol. Model.* **2007**, *13*, 631–642.
- (22) Wesolowski, T. A.; Chermette, H.; Weber, J. *J. Chem. Phys.* **1996**, *105*, 9182–9190.
- (23) Tran, F.; Weber, J.; Wesolowski, T. A. *Helv. Chim. Acta* **2001**, *84*, 1489–1503.
- (24) Wesolowski, T. A.; Morgantini, P.-Y.; Weber, J. *J. Chem. Phys.* **2002**, *116*, 6411–6421.
- (25) Jacob, C. R.; Neugebauer, J.; Visscher, L. *J. Comput. Chem.* **2007**, *29*, 1011–1018.
- (26) *ADF2008.01*; SCM, Theoretical Chemistry, Vrije Universiteit: Amsterdam, The Netherlands. <http://www.scm.com> (accessed May 26th, 2009).
- (27) Guerra, C. F.; Snijders, J.; te Velde, G.; Baerends, E. J. *Theor. Chem. Acc.* **1998**, *99*, 391–403.
- (28) te Velde, G.; Bickelhaupt, F. M.; Baerends, E. J.; Guerra, C. F.; van Gisbergen, S. J. A.; Snijders, J. G.; Ziegler, T. *J. Comput. Chem.* **2001**, *22*, 931–967.
- (29) Wesolowski, T. A.; Weber, J. *Chem. Phys. Lett.* **1996**, *248*, 71–76.
- (30) Bernard, Y. A.; Dulak, M.; Kaminski, J. W.; Wesolowski, T. A. *J. Phys. A: Math. Theor.* **2008**, *41*, 055302.
- (31) Ludeña, E. V.; Karasiev, V. V. Kinetic energy functionals: History, challenges and prospects. In *Reviews of Modern Quantum Chemistry*; Sen, K. D., Ed.; World Scientific Publishing: Singapore, 2002; Vol. 1.
- (32) Ernzerhof, M. *J. Mol. Struct.: THEOCHEM* **2000**, *501*, 59–64.
- (33) Karasiev, V. V.; Trickey, S. B.; Harris, F. E. *J. Comput.-Aided Mater. Des.* **2006**, *13*, 111–129.
- (34) Kirzhnits, D. A. *Sov. Phys. JETP* **1957**, *5*, 64.
- (35) Hodges, C. H. *Can. J. Phys.* **1973**, *51*, 1428–1437.
- (36) Perdew, J. P. *Phys. Lett. A* **1992**, *165*, 79–82.
- (37) Ou-Yang, H.; Levy, M. *Int. J. Quantum Chem.* **1991**, *40*, 379–388.
- (38) Lee, H.; Lee, C.; Parr, R. G. *Phys. Rev. A* **1991**, *44*, 768–771.
- (39) Becke, A. D. *Phys. Rev. A* **1988**, *38*, 3098–3100.
- (40) Perdew, J. P.; Wang, Y. *Phys. Rev. B* **1986**, *33*, 8800–8802.
- (41) Lacke, D. J.; Gordon, R. G. *J. Chem. Phys.* **1994**, *100*, 4446–4452.
- (42) Perdew, J. P.; Chevary, J.; Vosko, S.; Jackson, K. A.; Pederson, M. R.; Singh, D.; Fiolhais, C. *Phys. Rev. B* **1992**, *46*, 6671–6687.
- (43) Becke, A. D. *J. Chem. Phys.* **1986**, *84*, 4524–4529.
- (44) Perdew, J. P.; Burke, K.; Ernzerhof, M. *Phys. Rev. Lett.* **1996**, *77*, 3865–3868.
- (45) Perdew, J. P.; Burke, K.; Ernzerhof, M. *Phys. Rev. Lett.* **1997**, *78*, 1396.
- (46) Tran, F.; Wesolowski, T. A. *Int. J. Quantum Chem.* **2002**, *89*, 441–446.
- (47) Thakkar, A. J. *Phys. Rev. A* **1992**, *46*, 6920–6924.
- (48) Adamo, C.; Barone, V. *J. Chem. Phys.* **2002**, *116*, 5933–5940.
- (49) Zhao, Y.; Truhlar, D. G. *J. Chem. Theory Comput.* **2005**, *1*, 415–432.
- (50) Zhao, Y.; Truhlar, D. G. *J. Phys. Chem. A* **2005**, *109*, 5656–5667.
- (51) Grimme, S. *J. Comput. Chem.* **2004**, *25*, 1463–1473.
- (52) Zhao, Y.; Truhlar, D. G. *Phys. Chem. Chem. Phys.* **2005**, *7*, 2701–2705.
- (53) Amin, E. A.; Truhlar, D. G. *J. Chem. Theory Comput.* **2008**, *4*, 75–85.
- (54) Wesolowski, T. A.; Weber, J. *Int. J. Quantum Chem.* **1997**, *61*, 303–311.
- (55) Boys, S. F.; Bernardi, F. *Mol. Phys.* **1970**, *19*, 553–566.
- (56) Jacob, C. R.; Götz, A. W.; Bulo, R. E.; Beyhan, S. M.; Visscher, L. PyADF; VU University Amsterdam and ETH Zurich, 2007–2009.
- (57) Python. <http://www.python.org> (accessed May 26th, 2009).
- (58) Dulak, M.; Wesolowski, T. A. *Int. J. Quantum Chem.* **2005**, *101*, 543–549.
- (59) Baerends, E. J.; Ellis, D.; Roos, P. *Chem. Phys.* **1973**, *2*, 41–51.
- (60) Dunlap, B. I.; Connolly, J. W. D.; Sabin, J. R. *J. Chem. Phys.* **1979**, *71*, 3396–3402.
- (61) Jacob, C. R.; Beyhan, S. M.; Visscher, L. *J. Chem. Phys.* **2007**, *126*, 234116.
- (62) Mulliken, R. S. *J. Chem. Phys.* **1955**, *23*, 1833–1840.

CT9001784